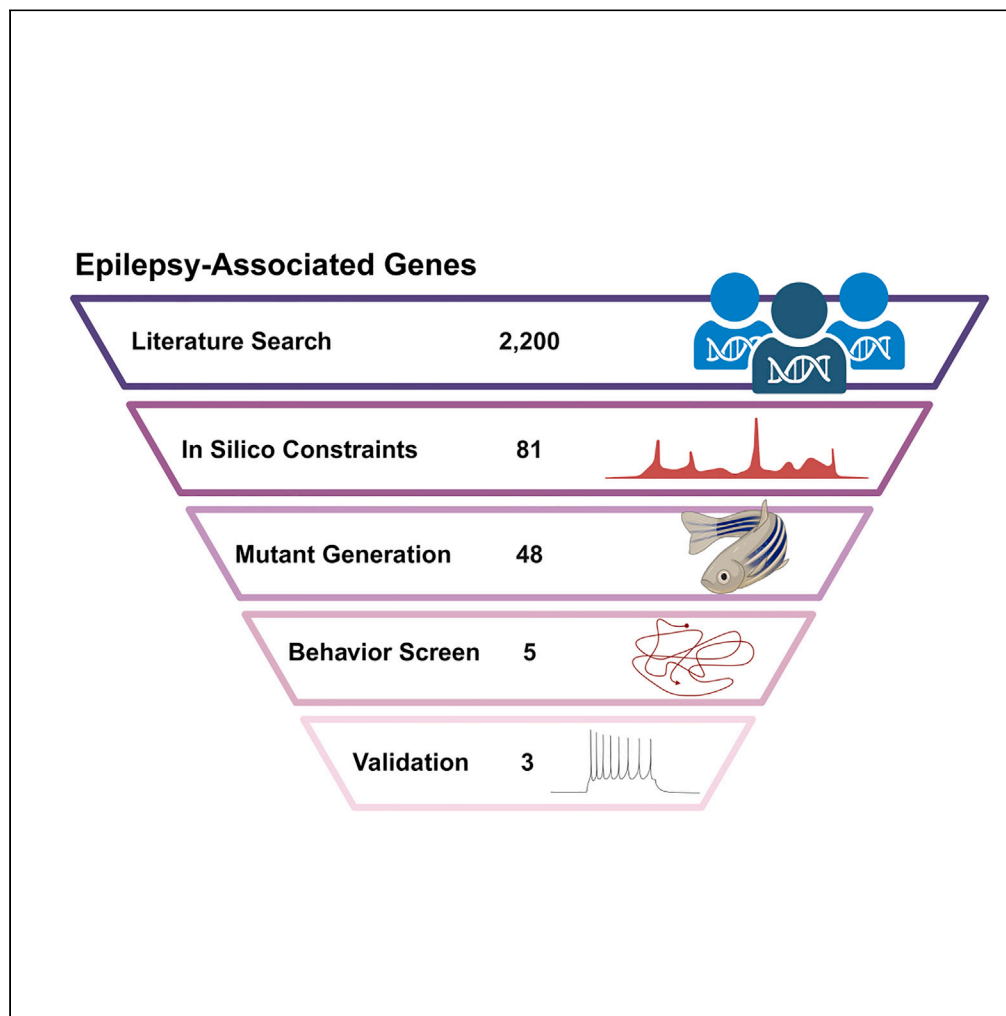**Article**

Zebrafish models of candidate human epilepsy-associated genes provide evidence of hyperexcitability

Christopher Mark LaCoursiere, Jeremy F.P. Ullmann, Hyun Yong Koh, ..., Alexander Rotenberg, Christopher M. McGraw, Annapurna H. Poduri

annapurna.poduri@childrens.harvard.edu

Highlights

Arfgef1, *kcnd2*, *kcnv1*, *ubr5*, and *wnt8b* zebrafish mutants display seizures

Abnormal electrical activity is detected in *kcnd2* and *wnt8b* mutant larvae

Arfgef1 and *wnt8b* mutants have decreased tectal inhibitory interneurons vs. wildtype

RNA-seq reveals convergent dysregulation across genetic mutants

Article

Zebrafish models of candidate human epilepsy-associated genes provide evidence of hyperexcitability

Christopher Mark LaCoursiere,[1,2] Jeremy F.P. Ullmann,[1,2] Hyun Yong Koh,[1,2,3] Laura Turner,[1,2] Cristina M. Baker,[1,2,4] Barbara Robens,[1,2] Wanqing Shao,[5] Alexander Rotenberg,[1,6,7,8] Christopher M. McGraw,[1,2,6,8] and Annapurna H. Poduri[1,2,6,8,9,10,*]

SUMMARY

Hundreds of novel candidate human epilepsy-associated genes have been identified thanks to advancements in next-generation sequencing and large genome-wide association studies, but establishing genetic etiology requires functional validation. We generated a list of >2,200 candidate epilepsy-associated genes, of which 48 were developed into stable loss-of-function (LOF) zebrafish models. Of those 48, evidence of seizure-like behavior was present in 5 (*arfgef1*, *kcnd2*, *kcnv1*, *ubr5*, and *wnt8b*). Further characterization provided evidence for epileptiform activity via electrophysiology in *kcnd2* and *wnt8b* mutants. Additionally, *arfgef1* and *wnt8b* mutants showed a decrease in the number of inhibitory interneurons in the optic tectum of larval animals. Further, RNA sequencing (RNA-seq) revealed convergent transcriptional abnormalities between mutant lines, consistent with their developmental defects and hyperexcitable phenotypes. These zebrafish models provide strongest experimental evidence supporting the role of *ARFGEF1*, *KCND2*, and *WNT8B* in human epilepsy and further demonstrate the utility of this model system for evaluating candidate human epilepsy genes.

INTRODUCTION

Epilepsy is a condition defined by recurrent, unprovoked seizures affecting 1% of the population, including 1 in 200 children,[1] with a lifetime prevalence of 1 in 26.[2] Major personal and societal impacts for people living with epilepsy include refractory seizures, neurodevelopmental and neuropsychiatric comorbidities, high epilepsy-related healthcare costs, and increased risk of sudden death.[3] Underlying etiologies are heterogeneous and include both acquired and genetic factors. Recent technological advancements in genetics research have enabled the characterization of numerous monogenic epilepsies,[4–6] collectively accounting for a substantial portion of otherwise clinically unexplained disorders.[7] Through collaborative efforts to study the role of genetics in the epilepsies, as well as those of individual laboratories, the number of genes associated with epilepsy has steeply risen to >2,000.[8–10] While a few well-powered, large studies have securely implicated novel genes in early onset epilepsy, many reports have revealed candidate genes that require validation,[11] both in additional patient cohorts and in experimental systems. Despite major progress in gene discovery, treatment for epilepsy continues to be empiric and often unsuccessful, with at least one-third of patients with epilepsy continuing to experience seizures despite treatment with anti-seizure medications (ASMs). The development of rational treatments for monogenic epilepsies requires clinically relevant functional models to dissect gene-specific epileptogenic mechanisms and develop targeted therapies.[12]

Characterization of the numerous, heterogeneous genetic epilepsies poses a challenge, as many distinct models are needed to study the wide range of biological processes that, when disrupted, result in circuit dysfunction and hyperexcitability. An additional challenge stems from the fact that these models of central nervous system (CNS) dysfunction may result in broad neurodevelopmental phenotypes or potentially only transient episodic phenotypes akin to human seizures.[13] Overcoming these challenges require *in vivo* models and multiple diverse modalities to characterize normal and disease states. Conventional epilepsy models, such as rodent, are expensive and time-consuming to

[1]F.M. Kirby Neurobiology Center, Department of Neurology, Boston Children's Hospital, Boston, MA 02115, USA
[2]Epilepsy Genetics Program, Department of Neurology, Boston Children's Hospital, Boston, MA 02115, USA
[3]Departments of Neuroscience and Pediatrics, Division of Neurology and Developmental Neuroscience, BCM, Houston, TX 77030, USA
[4]Kavli Institute for Systems Neuroscience, Norwegian University of Science and Technology, 7034 Trondheim, Norway
[5]Research Computing, Department of Information Technology, Boston Children's Hospital, Boston, MA 02115, USA
[6]Department of Neurology, Harvard Medical School, Boston, MA 02115, USA
[7]Division of Epilepsy and Clinical Neurophysiology, Department of Neurology, Boston Children's Hospital, Boston, MA 02115, USA
[8]Department of Neurology, Massachusetts General Hospital, Boston, MA 02114, USA
[9]Broad Institute of Harvard and MIT, Cambridge, MA 02142, USA
[10]Lead contact
*Correspondence: annapurna.poduri@childrens.harvard.edu
https://doi.org/10.1016/j.isci.2024.110172

generate and, further, are not guaranteed to display phenotypes relevant to human epilepsy, including the most basic phenotype of seizures.[14] Zebrafish (*Danio rerio*) are an increasingly employed epilepsy model because of their high genetic homology to humans, large clutch sizes (100–400 embryos), inexpensive husbandry costs, and the ease with which their small, transparent larvae readily allow for morphologic phenotyping.[15] The relevance of zebrafish to epilepsy disease modeling and drug discovery has been demonstrated by the presence of seizure-like events and electrophysiological abnormalities similar to those observed in human epilepsy,[16] as well as translation from drug screens in genetic models of *SCN1A*-related epilepsy, a prototypical genetic epilepsy with childhood onset and associated cognitive comorbidities and risk of sudden death.[17]

Motivated by burgeoning human genetics discoveries, we present the results of a literature-based search for novel genes associated with developmental epilepsies, assessment for suitability of modeling in zebrafish, CRISPR model generation for 81 genes, and automated seizure detection followed by validation and characterization of the 5 most promising models. Our pipeline and results further the priorities of the epilepsy genetics community for pre-clinical, precision medicine approaches to diagnose and treat genetic epilepsies.

RESULTS

Selection of candidate human epilepsy-associated genes for modeling in zebrafish

To select genes suitable for modeling epilepsy in zebrafish, we first generated a master list of >2,200 unique epilepsy-related genes consolidated and vetted by the neurologists and genetic counselors of our Epilepsy Genetics Program (Figure 1A.i). This list was refined to include genes that are intolerant to missense variation (Z score > 3) or loss-of-function (LOF) (probability of LOF intolerance, pLI > 0.9) according to metrics from the Exome Aggregation Consortium database[18] and subsequently the gnomAD database.[19] Final *in silico* refinement included genes with zebrafish-human homology of at least 60% with no previously established animal model. A small selection of candidates not meeting all metrics, but with additional evidence of pathogenicity from exome data analyzed through the Epilepsy Genetics Program, were also included (Figure 1A.ii; Table S1). This resulted in a list of 81 genes with highly heterogenous molecular functions (Figure 1B; Table S1).

All refined genes were targeted with multiple single guide RNAs (sgRNAs) (Table S1) to develop F_0 crispants. A single mutation (two if the zebrafish gene is duplication) was chosen per gene that was predicted to produce an LOF insertion or deletion (indel) in a protein-coding region, as confirmed by Synthego ICE analysis. Given preliminary >90% cutting efficiency, a shotgun gene targeting approach,[20] and a gene list highly intolerant to LOF, any transcript that failed to transmit (>8 pools of 5 F_1 larvae) to F_1 germline was assumed likely embryonic lethal. Additionally, F_1 fish that did not result in viable heterozygous (HET) in-cross (after >10 breeding opportunities) and thus did not provide F_2 offspring for downstream analysis were not pursued further. In total, 48 candidates led to viable models subjected to further evaluation (Figure 1A.iii). Functional validation of suitable candidates began with three larval swim paradigms (detailed in STAR Methods), which implicated 5 of 48 mutants with classic larval zebrafish seizure (stage SII) swim patterns (Figure 1A.iv). Indel mutations in those 5 lines (*arfgef1*, *kcnd2*, *kcnv1*, *ubr5*, and *wnt8b*) are depicted in Figure 1C. Notably, 3/5 mutations were in-frame and not predicted to result in truncation or complete knockout (KO) as confirmed by Sanger sequencing. *Arfgef1* models contain a 10 base pair deletion and 4 base pair insertion resulting in a p.L367S missense as well as a two amino acid deletion at p.E368_E369. *Kcnd2* editing resulted in an in-frame 3-base pair deletion at the evolutionarily conserved amino acid p.M375 (Figure 1C), while *wnt8b* mutants contain a ten base pair deletion resulting in splice site removal and deletion of two amino acids at p.S79_R80. Indels in *kcnv1* and *ubr5* models are early truncating frameshift mutations. (Figure 1C; Table S2). Ungenotyped mutants assayed in behavior paradigms were predicted to contain the reported single mutation per paralog (Table S2), with a Mendelian pattern expected from an HET ✕ HET cross. These five behaviorally positive mutants were then subjected to downstream assays to provide additional evidence of hyperexcitability. (Figure 1A.v).

Seizure-like swim patterns provide initial evidence of gene-disease association in 5 mutant lines

Initial F_2 screening was conducted by recording and analysis of locomotion with analysis of swim patterns for seizure-like patterns at 5dpf. No obvious increase in normal beat and glide swim (SI) activity was observed in any ungenotyped mutant assays (Table S2). Previous studies[16] have shown that classic swirling swim patterns representing seizure events (SII) can be followed by a postictal-like decrease in movement. Detection of SII events may be limited using average velocity to screen for abnormal behavior due to periods of prolonged inactivity following the seizure events. Therefore, we developed parameters to identify discrete SII events, and SII detection was automated from video files with a classifier algorithm (detailed in STAR Methods). A "positive" SII result for a given gene indicates an increased binomial probability of SII events in mutant populations compared to the wild-type (WT) SII population. We observed that 5 candidate gene models displayed statistically increased probability of SII events. Of the five genes with increased SII activity *wnt8b* was the only mutant that showed an abnormality in SI swim pattern, which was in fact a decrease (Table S3).

We observed evidence of seizure events in 5 mutant lines: *arfgef1*, *kcnd2*, *kcnv1*, *ubr5*, and *wnt8b*. Specifically, we observed increased binomial probability of SII seizure events in mutants vs. WT larvae in at least one of three paradigms (spontaneous, light-induced, and subthreshold PTZ-induced). Both *kcnv1* HET and *kcnv1* homozygous (HOM) larvae displayed spontaneous seizures, with a total of 19 SII seizure events across all paradigms (Figure 1D). There was a total of 8 SII seizure events in *kcnd2* HET larvae across all paradigms. *Arfgef1* HOM mutants showed a significant increase in light induced SII seizure events (average 8 total SII events vs. 0 in WT). *Ubr5* HET mutants, but interestingly not *ubr5* HOM mutants, displayed increased spontaneous seizure-like events vs. WT. Similarly, *wnt8b* HOM mutants displayed light paradigm induced SII seizure (Figure 1D). We noted that several WT larvae generated from both *wnt8b* and *ubr5* crosses had higher tendency to show SII seizures than stock WT data (Table S2), suggesting the need for comparisons to be made with WT sibling controls. Together these
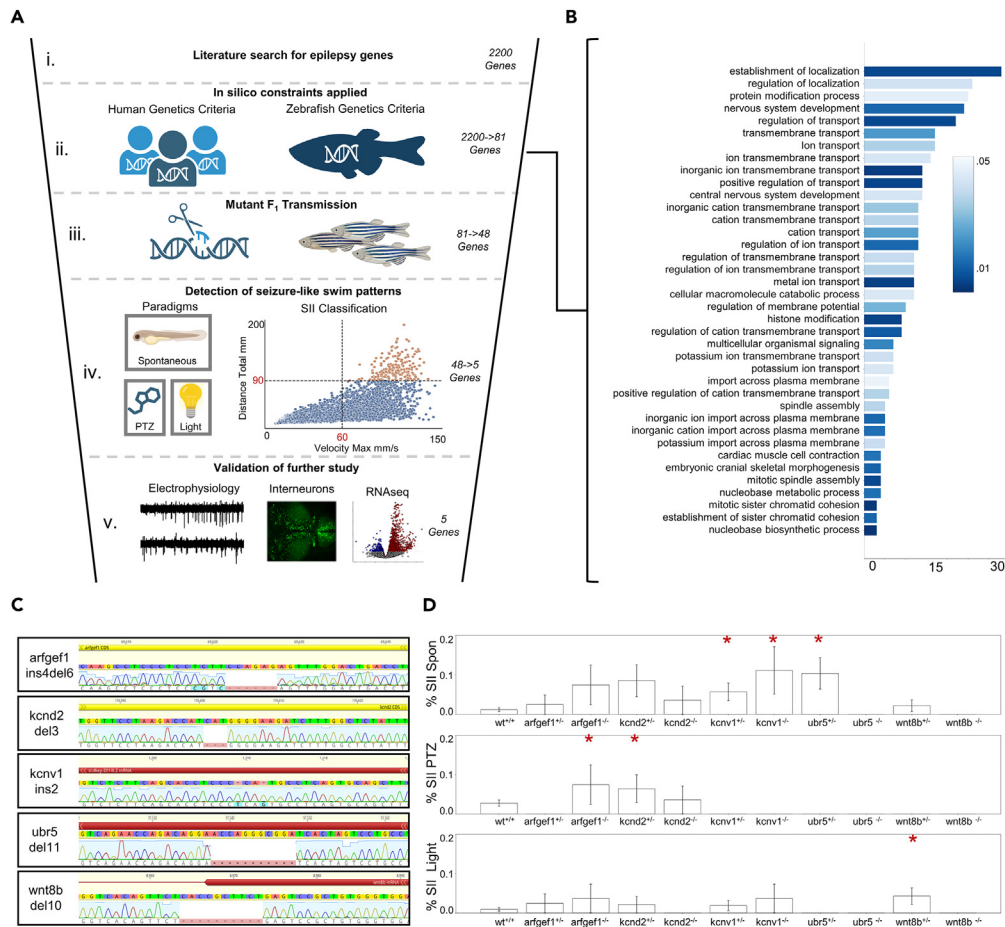
Figure 1. Overview of evaluation of candidate human epilepsy genes in zebrafish models

(A) Graphical depiction of primary F_2 screening method including: (i) initial gene identification through literature search; (ii) application of in silico constraints; (iii) generation of initial crispants and stable F2 mutants; (iv) detection of seizure-like swim patterns in either a spontaneous, light-provoked, or subthreshold PTZ assay; and (v) characterization of mutant lines that displayed SII seizure events via local field potentials, quantifying *dlx*-GFP expressing inhibitory interneurons and RNA-seq.

(B) 48 genes for which we generated surviving crispants and stable mutant lines represent heterogeneous Gene Ontology (GO) categories of biological processes.

(C) Schematic of homozygous mutations found in the five genes meeting criteria for positive seizure-like swim patterns.

(D) Results from three paradigms suggesting hyperexcitability based on swim patterns. Paradigms included a 1h spontaneous recording, a light provoked recording and a subthreshold PTZ provoked paradigm. Mutant larvae exhibited limited SI-like behavior as shown by mean velocity, but 5 mutant alleles showed an increase in the proportion of larvae with at least one SII event. Statistical significance for SI behavior was determined by Kruskal-Wallis tests with Dunn multiple comparisons while significance of SII events was determined by the binomial probability of SII events compared to the expected value from the population proportion. Significance was determined within a 95% confidence interval, *$p < 0.05$, **$p < 0.01$, ***$p < 0.001$. Data are represented as proportional mean $\pm$ STD. Candidate gene list and information available in Table S1. Behavior n per gene and genotype is available in Table S2. Additional information available in Table S3. Figure (A) was created with BioRender.com.

data demonstrate that SII behavioral seizures occur only rarely as assessed by our experimental paradigms, and they implicate 5 genes from our primary F_2 screen for further characterization.

Additional characterization of hyperexcitability

Of the 5 genes demonstrating seizures using high-throughput detection of SII swim patterns, 2 had models that additionally displayed abnormal and hyperexcitable electrophysiological activity. Recordings were conducted in the optic tectum, a conventional location for recording that allows demonstration of epileptiform activity in larval zebrafish[21–23] (Figures 2A–2C). The 5 candidate genes were assayed (HET and HOM mutants) and compared to WT sibling controls 5–6 days post fertilization (dpf) during a 22-min window of a half-hour recording to allow for initial acclimatization. Mutant larvae displayed a range of abnormal spiking including an increase in spike count and spike
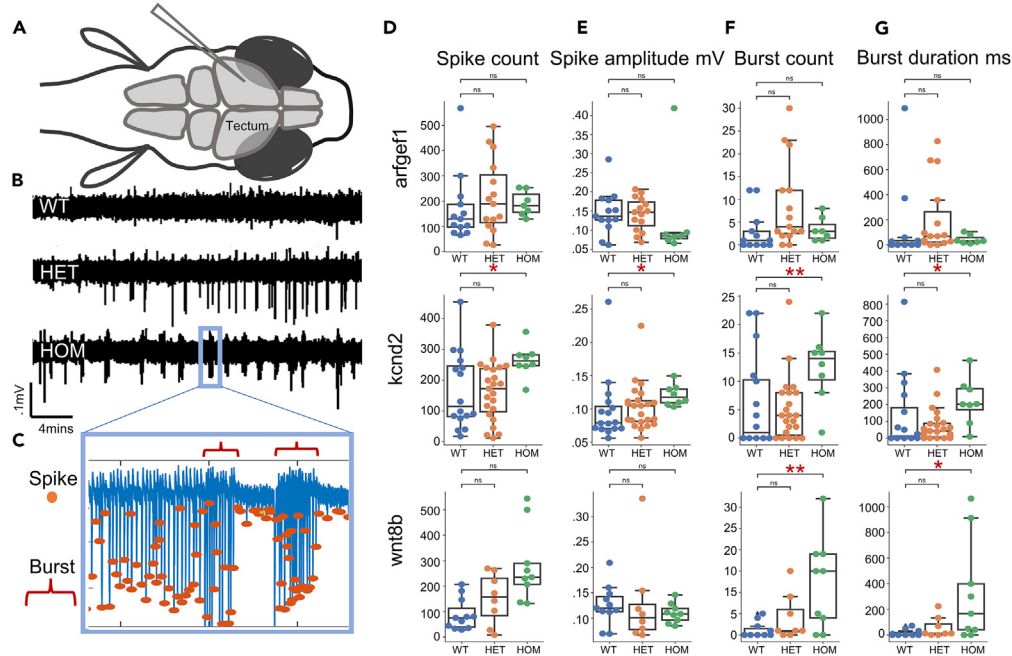
Figure 2. Epileptiform activity of larval tectum in electrophysiological recordings

(A) Schematic representation of larval zebrafish LFP recordings.

(B) Exemplary LFP recordings from kcnd2 larvae showing a dose sensitive increase in spike amplitude, frequency, distribution, and bursting.

(C) Exemplary recordings of spike count, amplitude and burst count and duration.

(D) Spike count quantification is increased *kcnd2* and *wnt8b* HOM larvae compared to WT sibling controls.

(E) Spike amplitude is increased in HOM kcnd2 larvae compared to WT sibling controls.

(F and G) Burst count and duration increased in *kcnd2* and *wnt8b* HOM compared to WT sibling controls. *Arfgef1* WT: *n* = 12, HET: *n* = 15, HOM *n* = 7; *kcnd2* WT: *n* = 16, HET: *n* = 23, HOM *n* = 8; *wnt8b* WT: *n* = 11, HET: *n* = 8, HOM *n* = 9. Statistical significance was determined by Kruskal-Wallis test with Dunn multiple comparisons, *$p < 0.05$, **$p < 0.01$, ***$p < 0.001$. For D, E, F, and G, data are represented as median $\pm 1.5*IQR$. Additional information available in Table S3.

amplitude (Figures 2D and 2E). We observed a wide range of epileptiform-like values in WT groups in all parameters assayed, consistent with the necessity for WT sibling control comparisons in local field potential (LFP) experiments as previously described.[21] *Kcnd2* mutants proved to have the strongest evidence of hyperexcitability with an increase in average spike rate and amplitude as well as increased bursting duration and frequency. All parameters indicated a dose dependence, with the severity of phenotypes increasing from HET to HOM. *Wnt8b* mutants also exhibited a dose-dependent increase in hyperexcitability in spike rate, burst count, and burst duration, with HOM mutants more severely affected than HET clutch mates (Figures 2F and 2G). The *arfgef1* (Figures 2G–2E), *ubr5*, and *kcnv1* mutants did not display statistically significant abnormalities in LFP measurements (Table S3).

Reduced interneuron number in candidate epilepsy gene models

To assess whether abnormal larval tectal development could contribute to the SII seizures and hyperexcitable phenotypes observed in LFP experiments, we quantified inhibitory interneurons in WT, HET, and HOM larvae (Figure 3A). No qualitative difference in the distribution of inhibitory interneurons was observed between mutant and WT forebrain, tectum, and hindbrain of age-matched 5 dpf larvae. Dense clusters aggregated near anatomical boundaries and the midline and dispersed radially with no gross differences between mutants and WT sibling controls (Figure 3B). Regional quantification of larval tectum was isolated and quantified to directly probe development of observed hyperexcitable structures. Of the 3 candidate genes with increased excitation from LFP experiments, 2 showed a significant reduction in inhibitory interneurons: *arfgef1* and *wnt8b*. Both genes' models showed a decrease in HET interneuron quantity in the larval tectum followed by a more dramatic decrease in HOM larvae (Figure 3C). *Kcnv1* and *kcnd2* models showed no indication of GABAergic interneuron reduction (Table S3).

Transcriptomic differences in zebrafish epilepsy models

Given the heterogeneity of genetic causes of epilepsy but the convergence of a hyperexcitability phenotype, transcriptomic patterns were assessed across the mutant zebrafish that showed structural or electrophysiological abnormalities to probe for convergent pathways that might lead to hyperexcitability. Larval heads were dissected and pooled by genotype and assayed via RNA sequencing (RNA-seq) (Figure S1A). We identified thousands of differentially expressed genes (DEGs) within mutants as compared to WT sibling controls (Figures 4A.i–4A.iii). The most striking differences were seen in candidates with strong findings via LFP; *kcnd2* and *wnt8b* (Figures 4A.ii
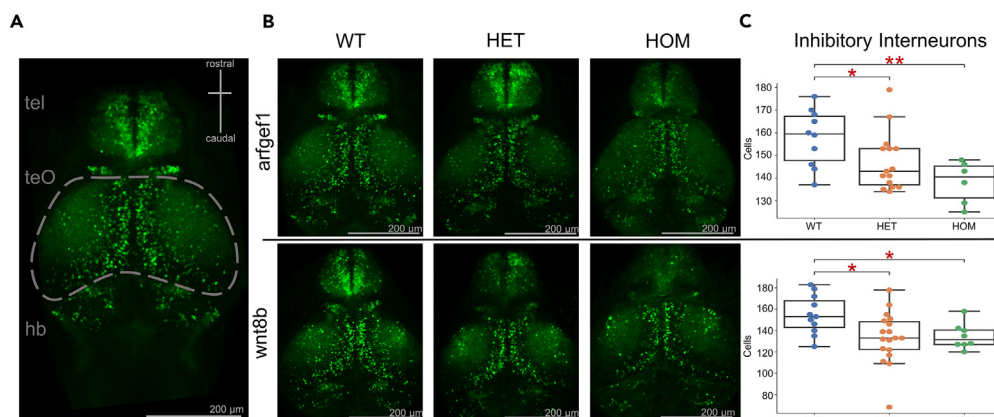
Figure 3. A dose-dependent decrease in the number of interneurons in a subset of zebrafish mutant lines, *arfgerf1* and *wnt8b*

(A) Schematic representation of larval zebrafish brain gross anatomy highlighting the optic tectum.

(B) Exemplary images of *arfgef1* and *wnt8b* mutant allele combinations.

(C) Dose-dependent decrease in inhibitory interneurons in *arfgef1* and *wnt8b* mutants compared to WT sibling controls. tel, telencephalon; teO, optic tectum; hb, hindbrain. *Arfgef1* WT: $n = 10$, HET: $n = 15$, HOM $n = 6$; *wnt8b* WT: $n = 11$, HET: $n = 18$, HOM $n = 8$ Statistical significance was determined by Kruskal-Wallis test with Dunnett's multiple comparisons, $*p < 0.05$, $**p < 0.01$, $***p < 0.001$. Data are represented as median $\pm 1.5*IQR$. Scale bar is 200 μm. Additional information available in Table S3.

and 4A.iii). Considering DEGs for only Hom vs. WT for each mutant line, data from *wnt8b* mutant larvae displayed the most dysregulation, followed by *kcnd2* and finally *arfgef1* (Figures 4B.i–4B.iii). Only the mutant *arfgef1* HOMs show a significant reduction in mutant gene transcription as compared with WT (Figure 4A.i). Of those genes that were dysregulated in mutant lines, DEG co-occurrence from our previously published EPGP epilepsy gene list[11] was seen in the top twenty most significantly dysregulated genes in 2 HOM mut lines. These genes include *atp8a2* in *arfgef1* mutants (Figure 4C.i) as well as *col4a1* and *grin1b* in *wnt8b* mutants (Figure 4C.iii). When considering all co-occurrence between mutant line DEGs and the EPGP gene list, the highest number was seen in *kcnd2* ($n = 5/1443$) and *wnt8b* ($n = 298/1443$) mutants. However, when the total number of DEGs was taken into consideration, we did not observe an enrichment of the EPGP gene list within the DEGs, nor did we observe an enrichment of DEGs within the EPGP gene list for any mutants (Figure S1B). Interestingly, we observed transcriptional biomarkers for neuronal activity, immediate-early genes (IEGs), in the mutant lines with hyperexcitability LFP recordings. Dysregulation of *npas4a*, *npas4b*, *erg1*, *fosab*, and *nr4a1* was seen in mutant *wnt8b* (Figure 4D.i) fish and *fosab*, *erg1*, and *npas4b* in *kcnd2* (Figure 4D.ii) mutants. All IEG expression was significantly downregulated, consistent with chronic epilepsy as opposed to the upregulation observed after acute seizure induction.[24–26] Models with no significant findings from LFP also showed no significant IEG DEGs (Figures 4C–4E.ii). The highest number of co-occurrences of DEGs between mutant lines was also seen between *kcnd2* and *wnt8b* mutants while minimal co-occurrence was seen between *arfgef1* and *kcnd2* or *wnt8b* (Figure S1C).

Pathway analysis of dysregulated genes was particularly remarkable for *kcnd2* and *wnt8b* mutants (Figures 4E.ii and 4E.iii), with many Gene Ontology (GO) terms involved in axon development and synapse formation dysregulated, as has been reported in the context of human epileptic brain tissue.[27] *Arfgef1* mutants showed enrichment for genes related to neurotransmitter transport (Figure 4E.i).

DISCUSSION

As genomic sequencing continues in research studies and in the clinical setting,[28] new potential candidate genes are being identified on an on-going basis. For epilepsy, as clinical sequencing guidelines advocate for a genome-wide approach, there are numerous possible findings each time a patient is tested and an ever-growing number of candidate genes emerging for human epilepsy.[11] There is thus a growing need for experimental models to provide evidence to support the role of these candidate genes in human disease; a first step toward precision diagnosis and treatment. Knowing the potential of the zebrafish system to model key epilepsy-related features, we focused on a subset of candidate epilepsy genes that are amenable to study in the zebrafish system. We evaluated 48 zebrafish models for epilepsy-related phenotypes—first with a high-throughput behavioral screen to identify models with seizure-like swim patterns and then using local field potential recordings to evaluate for electrophysiological abnormalities and then evaluation for structural and gene expression abnormalities. We provide aggregate evidence that supports a role of the human orthologs of *arfgef1*, *kcnd2*, *kcnv1*, *ubr5*, and *wnt8b* in human epilepsy, with strongest evidence for *arfgef1*, *kcnd2*, and *wnt8b*. ARFGEF1's human disease association has been linked to developmental delay, variable brain malformations, and early onset refractory epilepsy.[29] Since initial generation of our candidate gene list and models, *Arfgef1* mouse models have been shown to have a decreased latency to tonic-clonic seizures in both a PTZ-provoked and electroconvulsant threshold models,[30] adding further evidence in support of this gene's role in human epilepsy. Human alleles in KCND2, with predicted gain and loss of function, have been associated with global developmental delay in one report[31] and with tonic-clonic seizures in a pair of monozygotic twins in another.[32] WNT8B's location at human chromosome 10q24 has raised the possibility that this gene plays a role in the pathogenesis of disorders associated with this locus, including glioblastoma multiforme, spinocerebellar ataxia, and focal epilepsy.[33]
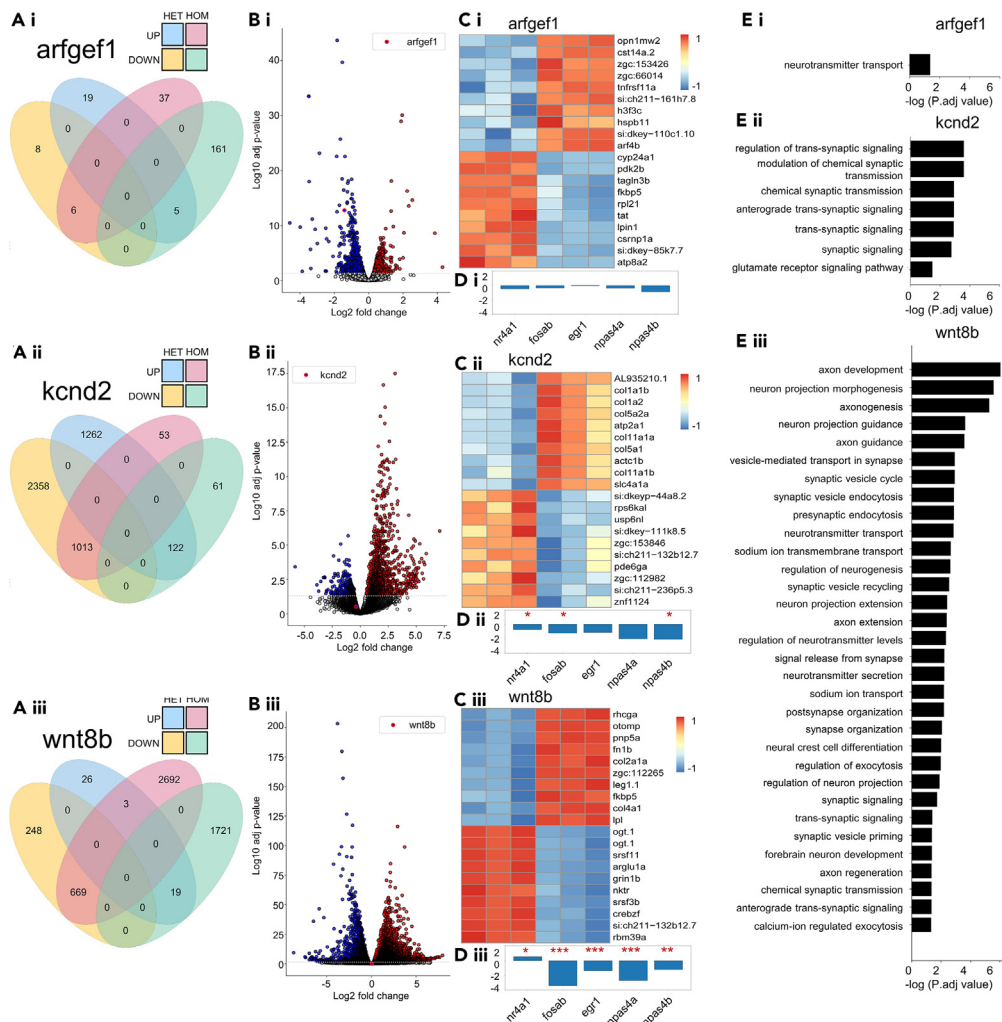
Figure 4. Mutants show dysregulation and coincidence, among phenotypically similar mutants, of epilepsy associated genes and ontologies

(A.i–A.iii) Venn diagram of the total number differentially expressed genes (DEGs) per mutant genotype.

(B.i–B.iii) Volcano plot of HOM vs. WT DEG's per mutant genotype.

(C.i–C.iii) The top twenty most up and down regulated genes in homozygous mutants versus control.

(D.i–D.iii) HOM vs. WT mutants effect size estimation of differential immediate-early gene transcription. padj < 0.05, *$p < 0.05$, **$p < 0.01$, ***$p < 0.001$.

(E.i–E.iii) Selective and possibly explanatory GO terms from HOM vs. WT DEGs. Additional information available in Figure S1.

Our approach was to prioritize and model genes, leveraging human sequencing data from affected and control populations, efficient and accurate CRISPR guide design and delivery into 1-cell zebrafish zygotes, followed by high-throughput behavioral swim pattern assays to identify larval zebrafish models with readily detectable seizure events and then lower throughput electrophysiological, histopathological, and RNA expression studies. There are advantages and limitations to each of these approaches, and we acknowledge that in pursuit of initial high throughput and of the lowest possible false-positive rate, we may have failed to demonstrate evidence of an association with epilepsy for some genes that in time will be found to have a strong gene-disease association. Conversely, any gene whose model survived to be evaluated and displayed phenotypic abnormalities consistent with seizures and abnormal network properties can be considered to have evidence to implicate that gene in epilepsy.

We had initially sought to model 81 candidate epilepsy genes that are intolerant to variation in the human population and that share good homology between human and zebrafish. We achieved 48 viable models, leaving the possibility that some of the other 33 may be disease-associated but that LOF in zebrafish is not compatible with survival. Our method of assaying swim behavior as an initial screening tool affords face validity and efficiency but has some limitations. The zebrafish SII behavioral seizure event is comparable to the tonic and/or tonic-clonic seizures observed in many patients with epilepsy and provides an objective, quantifiable measure that can be assayed in initial studies to implicate genes in epilepsy, as we have done, and in pre-clinical compound screening studies. We appreciate that our initial behavioral screen relies on intact swimming ability and may therefore not provide evidence of abnormality for every gene that will ultimately show an association

with epilepsy. The 5 models showing seizure events were then assayed using conventional, albeit lower throughput, electrophysiology (LFP) recording to assess for evidence of network hyperexcitability within the brain. This investigation approximates the electroencephalogram (EEG) conducted in individuals with suspected seizures as part of their epilepsy evaluation. Some zebrafish models, such as *scn1lab*, have been shown to display frequent SII events and a robust hyperexcitable LFP pattern.[17] Given the relatively small numbers of seizure events in the genetic models we generated, large numbers of larvae were required to conduct blinded experiments, and there are likely false negatives among the lines we designated as not having seizure events. We employed a binomial statistical method to compare populations of larvae (WT, HET, and HOM for each gene) since this method is suitable in the setting of rare events. Given the transient and often very rare nature of seizure events, hyperexcitable phenotypes could have been missed in behavioral and electrophysiology recordings. As previously reported in a large-scale assessment using extensive electrophysiological data, not all zebrafish models of even known epilepsy-associated genes will necessarily display abnormalities using conventional LFP methods.[21]

Animal models of some of the epilepsy-associated genes from our initial gene list have been described since the inception of this project. One study reports that *stxbp1a* and *stxbp1b* zebrafish KO models resulted in reduced locomotion and early lethality or spontaneous seizure, respectively.[34] We implemented a 6-guide strategy for generating a double KO mutant, with 4 of these guides targeting *stxpb1a*. Four guide redundant gene targeting has been shown to result in biallelic KO in up to 98% of zebrafish F_0 crispants.[35] None of the *stxbp1* models that we generated survived to the F_1 stage, which given our targeting strategy, could have been the result of early lethality from *stxbp1a* KO. Additionally, *chd2* morpholino knockdown (KD) zebrafish have been shown to have abnormal morphology, including uninflated swim bladder, and hyperexcitable activity via LFP.[36] Our *chd2* crispants survived and were bred to the F_1 stage but showed no evidence of SII swimming. This may be due to a reduction in swimming capacity from uninflated swim bladder and independent of abnormal electrical activity. Along these lines, a previous report showed mutant *arx* larvae to have hypoactive movement with seizure-like activity via LFP,[21] suggesting that low swim velocities and lack of SII events should not exclude the possibility of a gene's causative role in epileptogenesis, thereby highlighting a limitation of our sequence from high-throughput to low-throughput methods.

Interestingly, for the genes *kcnd2* and *wnt8b*, seizure-like swim patterns (SII events) were observed in only the HET mutants. We hypothesize that this may be because HOMs had such severe neurodevelopmental disruption that they were hypomotile, such as previously reported finding in *chd2* and *stxbp1* mutants, while HETs were only partially affected and thus still able to swim and generate SII events. We note, however, that HOM *kcnd2* and HOM *wnt8b* larvae display abnormal electrophysiological (LFP) findings, suggesting that they also have hyperexcitable network activity present and detectable in the LFP assay that does not require intact swimming movement and is in fact conducted in non-motile paralyzed larvae.

There are a range of reports suggesting the possibility of off-target effects associated with the CRISPR-Cas9 gene editing system in zebrafish. With these in mind, our experimental method was specifically designed to mitigate this possibility by rigorous *in silico* design, the generation of stable F_1 HETs via outcross, and the specificity of phenotype from a reverse genetic screen. Experiments in non-CRISPR-edited WT larvae show some, albeit rare, seizure-like activity as seen with our binomial behavior methods and as previously reported in larval LFP recordings.[21] The presence of rare hyperexcitable finding in our WT sibling controls is unlikely due to off-target effects but rather similar to the non-CRISPR-edited WT findings and the non-zero rate of human EEG abnormalities in the absence of epilepsy. Furthermore, the use of WT larvae resulting from HET × HET in-cross controls for the presence of any off-target mutations because inheritance should be similarly present across all genotypes resulting from such a cross.

There is a possibility that any given gene may exert development effects at later stage than we are studying. Further, there is a possibility that any epilepsy-associated genes may play a less significant or slightly different role in zebrafish but remain a monogenic cause of or contributor to epilepsy in humans. Certainly, more complex assays for defects in learning and memory can be undertaken in zebrafish, though this requires raising the fish to an older age and is not conducive to an early larval stage screen and was thus out of the scope of our present study. Future studies using more mature zebrafish, including models of some of the genes that did *not* display evidence of hyperexcitability in our larval models, may identify additional genes important for neurodevelopment and disease.

In some of the lines identified as having SII events, we demonstrated features pointing to potential mechanisms involved in generating or maintaining hyperexcitable brain networks, including decreased interneuron number in *arfgef1* and *wnt8b*. We and others have observed a comparable reduction of interneuron number in other genetic epilepsy and neurodevelopmental models.[37,38] Further, when we evaluated for convergent mechanisms using mRNA expression studies, we identified abnormal IEG expression and dysregulation in genes related to axon development, synapse formation, and neurotransmitter transport. Transcriptional dysregulation of pooled mutants, from lines that had displayed evidence of hyperexcitability via LFP (*kcnd2* and *wnt8b*), showed patterns consistent with those previously associated with chronic epilepsy. This is likely because all fish within the pool had constitutively low IEG expression and/or an attenuated facultative expression response to neuronal firing. IEG activation is a rapid response (peak expression can be within as little as 30 min)[39] to neuronal firing and seizure is often a rare and transient event. Therefore, if fish were having chronic seizures prior to 5 dpf, including electrographic events such as those we have detected via LFP recording, more larvae within a pool would be expected to display a "chronic" seizure pattern with low IEG expression.

We note some additional considerations related to the generation of CRISPR-Cas9-based gene editing. While the design of this CRISPR-mediated reverse genetic screen was intended to create out-of-frame indels, similar to a previously described zebrafish screen of established catastrophic epilepsy genes,[21] it did not guarantee generation of KO models. Interestingly, there is a growing body of evidence for increased transcription of compensatory genes in KO zebrafish models.[40–42] The mechanism for zebrafish KO compensation is still not completely understood, but nonsense-mediated decay (NMD) initiation from premature terminating codons (PTCs) has been shown to be necessary for an increase in adaptive gene transcription.[43] Of the 48 viable mutant lines 40 had predicted truncating mutations (Table S2), while

three—included among the five genes (*arfgef1*, *kcnd2*, and *wnt8b*) for which we demonstrate evidence for hyperexcitability—contained in-frame deletions also predicted to result in a loss-of-function effect. Interestingly, these three in-frame mutants proved to have the most striking evidence for epilepsy-like activity in either primary seizure detection or downstream assays. Additionally, it has been shown that far less transcriptional compensation occurs in HET PTC zebrafish models compared to HOM.[42] This phenomenon could potentially provide an additional explanation regarding the discrepancy between significant SII seizure event scores in the motion tracking paradigms of HET truncating alleles (Table S3) and the absence of corresponding findings in the corresponding HOM models. Indeed, three of five mutants with seizure events detected (*kcnd2*, *ubr5*, and *wnt8b*) had seizures solely in HET larvae, including two with the most striking findings in downstream assays.

Even considering the complexities of zebrafish compensatory mechanisms and the methodological limitations of primary F_2 behavioral screening, our high-throughput to low-throughput pipeline does yield evidence supporting an association with epilepsy for 5 genes, with hyperexcitability on LFP adding stronger evidence for 3 of those 5 genes and additional evidence from other modalities. Whereas our model of *kcnd2*, which encodes a potassium channel subunit, had the strongest evidence of hyperexcitability via LFP recording, our models of *arfgef1*[30,44] and *wnt8b*,[45] both associated with neurodevelopmental processes, showed a reduction in inhibitory interneurons. The approach we have employed, primary evaluation of behavioral seizures and abnormal electrical activity as well as structural and transcriptional abnormalities, attempts to accommodate the expected heterogeneity of the genes involved in human epilepsies by focusing on key core features of the network dysfunction common to all epilepsies. The rate of SII seizure detection (5/48) and hyperexcitability on LFP (2/48) among our *candidate* epilepsy gene models is not surprisingly slightly lower than the rate (8/40) in a recent publication characterizing established epilepsy genes in the zebrafish system.[21] Future studies may provide additional methods to screen and identify abnormalities in animal models of candidate genes for epilepsy. In the meantime, the models we have generated for *arfgef1*, *kcnd2*, *kcnv1*, *ubr5*, and *wnt8b* may now serve as pre-clinical models for drug screening, and the methods employed here can be applied to other emerging candidate genes for epilepsy.

Limitations of the study

We used the CRISPR-Cas9 gene editing system to generate acute crispant genetic models and then stable mutant lines, which carries a theoretical possibility of off-target effects with any genetic model generation. We have mitigated this effect by out-crossing the acute crispants such that any consistent effects would be attributable to the targeted gene.

We were able to generate 48 of the initially intended 81 zebrafish genetic models. Larvae from five of the surviving 48 mutant lines displayed behavioral swim patterns suggestive of seizures, and models of three of these genes had consistent additional abnormalities, either electrophysiological, interneuron number reduction, or both. As noted previously, methodological limitations make it highly likely that some of the mutant lines not displaying any of these abnormalities are actually "false negatives" and that we missed potentially hyperexcitable phenotypes in the other mutant lines. Mutants in our cohort would not continue past the behavioral screening stage if they had an increase in electrical activity that did not also cause an increase in swimming activity, for example, genetic mutants with central nervous system hyperexcitability but motor defects would not have pursued beyond the initial screening stage for behavioral seizures. Thus, the current study does not preclude any of the epilepsy associated genes without significant findings within a zebrafish model of epilepsy.

STAR★METHODS

Detailed methods are provided in the online version of this paper and include the following:

- KEY RESOURCES TABLE
- RESOURCE AVAILABILITY
  - Lead contact
  - Materials availability
  - Data and code availability
- EXPERIMENTAL MODEL AND STUDY PARTICIPANT DETAILS
- METHOD DETAILS
  - Generating a candidate epilepsy gene list
  - CRISPR guide design
  - Generation of stable zebrafish mutants
  - Zebrafish behavior paradigms
  - Local field potential recording
  - Imaging
  - RNA-Seq preparation
- QUANTIFICATION AND STATISTICAL ANALYSIS
  - Qualification and analysis of swim behavior
  - Local field potential analysis
  - RNA-Seq analysis

SUPPLEMENTAL INFORMATION

Supplemental information can be found online at https://doi.org/10.1016/j.isci.2024.110172.

ACKNOWLEDGMENTS

AUTHOR CONTRIBUTIONS

DECLARATION OF INTERESTS

REFERENCES

1. Cowan, L.D. (2002). The epidemiology of the epilepsies in children. Ment. Retard. Dev. Disabil. Res. Rev. 8, 171–181. https://doi.org/10.1002/mrdd.10035.

2. Hesdorffer, D.C., Logroscino, G., Benn, E.K.T., Katri, N., Cascino, G., and Hauser, W.A. (2011). Estimating risk for developing epilepsy: a population-based study in Rochester, Minnesota. Neurology 76, 23–27. https://doi.org/10.1212/WNL.0b013e318204a36a.

3. Berry, J.G., Poduri, A., Bonkowsky, J.L., Zhou, J., Graham, D.A., Welch, C., Putney, H., and Srivastava, R. (2012). Trends in resource utilization by children with neurological impairment in the United States inpatient health care system: a repeat cross-sectional study. PLoS Med. 9, e1001158. https://doi.org/10.1371/journal.pmed.1001158.

4. Veeramah, K.R., Johnstone, L., Karafet, T.M., Wolf, D., Sprissler, R., Salogiannis, J., Barth-Maron, A., Greenberg, M.E., Stuhlmann, T., Weinert, S., et al. (2013). Exome sequencing reveals new causal mutations in children with epileptic encephalopathies. Epilepsia 54, 1270–1281. https://doi.org/10.1111/epi.12201.

5. Epi4K Consortium; Epilepsy Phenome/Genome Project, Allen, A.S., Berkovic, S.F., Cossette, P., Delanty, N., Dlugos, D., Eichler, E.E., Epstein, M.P., Glauser, T., et al. (2013). De novo mutations in epileptic encephalopathies. Nature 501, 217–221. https://doi.org/10.1038/nature12439.

6. EuroEPINOMICS-RES Consortium; Epilepsy Phenome/Genome Project; Epi4K Consortium (2014). De novo mutations in synaptic transmission genes including DNM1 cause epileptic encephalopathies. Am. J. Hum. Genet. 95, 360–370. https://doi.org/10.1016/j.ajhg.2014.08.013.

7. Thomas, R.H., and Berkovic, S.F. (2014). The hidden genetics of epilepsy-a clinically important new paradigm. Nat. Rev. Neurol. 10, 283–292. https://doi.org/10.1038/nrneurol.2014.62.

8. Helbig, I., and Lowenstein, D.H. (2013). Genetics of the epilepsies: where are we and where are we going? Curr. Opin. Neurol. 26, 179–185. https://doi.org/10.1097/WCO.0b013e32835ee6ff.

9. Helbig, K.L., Farwell Hagman, K.D., Shinde, D.N., Mroske, C., Powis, Z., Li, S., Tang, S., and Helbig, I. (2016). Diagnostic exome sequencing provides a molecular diagnosis for a significant proportion of patients with epilepsy. Genet. Med. 18, 898–905. https://doi.org/10.1038/gim.2015.186.

10. Epi4K consortium; Epilepsy Phenome/Genome Project (2017). Ultra-rare genetic variation in common epilepsies: a case-control sequencing study. Lancet Neurol. 16, 135–143. https://doi.org/10.1016/S1474-4422(16)30359-3.

11. Koh, H.Y., Smith, L., Wiltrout, K.N., Podury, A., Chourasia, N., D'Gama, A.M., Park, M., Knight, D., Sexton, E.L., Koh, J.J., et al. (2023). Utility of Exome Sequencing for Diagnosis in Unexplained Pediatric-Onset Epilepsy. JAMA Netw. Open 6, e2324380. https://doi.org/10.1001/jamanetworkopen.2023.24380.

12. EpiPM Consortium (2015). A roadmap for precision medicine in the epilepsies. Lancet Neurol. 14, 1219–1228. https://doi.org/10.1016/S1474-4422(15)00199-4.

13. Poduri, A., and Lowenstein, D. (2011). Epilepsy genetics–past, present, and future. Curr. Opin. Genet. Dev. 21, 325–332. https://doi.org/10.1016/j.gde.2011.01.005.

14. Wang, W., and Frankel, W.N. (2021). Overlaps, gaps, and complexities of mouse models of Developmental and Epileptic Encephalopathy. Neurobiol. Dis. 148, 105220. https://doi.org/10.1016/j.nbd.2020.105220.

15. Zon, L.I. (1999). Zebrafish: a new model for human disease. Genome Res. 9, 99–100.

16. Hortopan, G.A., Dinday, M.T., and Baraban, S.C. (2010). Zebrafish as a model for studying genetic aspects of epilepsy. Dis. Model. Mech. 3, 144–148. https://doi.org/10.1242/dmm.002139.

17. Griffin, A., Hamling, K.R., Knupp, K., Hong, S., Lee, L.P., and Baraban, S.C. (2017). Clemizole and modulators of serotonin signalling suppress seizures in Dravet syndrome. Brain 140, 669–683. https://doi.org/10.1093/brain/aww342.

18. Lek, M., Karczewski, K.J., Minikel, E.V., Samocha, K.E., Banks, E., Fennell, T., O'Donnell-Luria, A.H., Ware, J.S., Hill, A.J., Cummings, B.B., et al. (2016). Analysis of protein-coding genetic variation in 60,706 humans. Nature 536, 285–291. https://doi.org/10.1038/nature19057.

19. Chen, S., Francioli, L.C., Goodrich, J.K., Collins, R.L., Kanai, M., Wang, Q., Alföldi, J., Watts, N.A., Vittal, C., Gauthier, L.D., et al. (2022). A genome-wide mutational constraint map quantified from variation in 76,156 human genomes. Preprint at bioRxiv. https://doi.org/10.1101/2022.03.20.485034.

20. Zhao, M., Gao, M., Xiong, L., Liu, Y., Tao, X., Gao, B., Liu, M., Wang, F., and Wei, D.Z. (2022). CRISPR-Cas Assisted Shotgun Mutagenesis Method for Evolutionary Genome Engineering. ACS Synth. Biol. 11,

1958–1970. https://doi.org/10.1021/acssynbio.2c00112.

21. Griffin, A., Carpenter, C., Liu, J., Paterno, R., Grone, B., Hamling, K., Moog, M., Dinday, M.T., Figueroa, F., Anvar, M., et al. (2021). Phenotypic analysis of catastrophic childhood epilepsy genes. Commun. Biol. 4, 680. https://doi.org/10.1038/s42003-021-02221-y.

22. de Calbiac, H., Dabacan, A., Marsan, E., Tostivint, H., Devienne, G., Ishida, S., Leguern, E., Baulac, S., Muresan, R.C., and Kabashi, E. (2018). Depdc5 knockdown causes mTOR-dependent motor hyperactivity in zebrafish. Ann. Clin. Transl. Neurol. 5, 510–523. https://doi.org/10.1002/acn3.542.

23. Hong, S., Lee, P., Baraban, S.C., and Lee, L.P. (2016). A Novel Long-term, Multi-Channel and Non-invasive Electrophysiology Platform for Zebrafish. Sci. Rep. 6, 28248. https://doi.org/10.1038/srep28248.

24. Kalinina, A., Krekhno, Z., Yee, J., Lehmann, H., and Fournier, N.M. (2022). Effect of repeated seizures on spatial exploration and immediate early gene expression in the hippocampus and dentate gyrus. IBRO Neurosci. Rep. 12, 73–80. https://doi.org/10.1016/j.ibneur.2021.12.008.

25. Calais, J.B., Valvassori, S.S., Resende, W.R., Feier, G., Athié, M.C.P., Ribeiro, S., Gattaz, W.F., Quevedo, J., and Ojopi, E.B. (2013). Long-term decrease in immediate early gene expression after electroconvulsive seizures. J. Neural. Transm. 120, 259–266. https://doi.org/10.1007/s00702-012-0861-4.

26. Houser, C.R., Huang, C.S., and Peng, Z. (2008). Dynamic seizure-related changes in extracellular signal-regulated kinase activation in a mouse model of temporal lobe epilepsy. Neuroscience 156, 222–237. https://doi.org/10.1016/j.neuroscience.2008.07.010.

27. Pfisterer, U., Petukhov, V., Demharter, S., Meichsner, J., Thompson, J.J., Batiuk, M.Y., Asenjo-Martinez, A., Vasistha, N.A., Thakur, A., Mikkelsen, J., et al. (2020). Identification of epilepsy-associated neuronal subtypes and gene expression underlying epileptogenesis. Nat. Commun. 11, 5038. https://doi.org/10.1038/s41467-020-18752-7.

28. Smith, L., Malinowski, J., Ceulemans, S., Peck, K., Walton, N., Sheidley, B.R., and Lippa, N. (2023). Genetic testing and counseling for the unexplained epilepsies: An evidence-based practice guideline of the National Society of Genetic Counselors. J. Genet. Couns. 32, 266–280. https://doi.org/10.1002/jgc4.1646.

29. Thomas, Q., Gautier, T., Marafi, D., Besnard, T., Willems, M., Moutton, S., Isidor, B., Cogné, B., Conrad, S., Tenconi, R., et al. (2021). Haploinsufficiency of ARFGEF1 is associated with developmental delay, intellectual disability, and epilepsy with variable expressivity. Genet. Med. 23, 1901–1911. https://doi.org/10.1038/s41436-021-01218-6.

30. Teoh, J., Subramanian, N., Pero, M.E., Bartolini, F., Amador, A., Kanber, A., Williams, D., Petri, S., Yang, M., Allen, A.S., et al. (2020). Arfgef1 haploinsufficiency in mice alters neuronal endosome composition and decreases membrane surface postsynaptic GABA(A) receptors. Neurobiol. Dis. 134, 104632. https://doi.org/10.1016/j.nbd.2019.104632.

31. Zhang, Y., Tachtsidis, G., Schob, C., Koko, M., Hedrich, U.B.S., Lerche, H., Lemke, J.R., van Haeringen, A., Ruivenkamp, C., Prescott, T., et al. (2021). KCND2 variants associated with global developmental delay differentially impair Kv4.2 channel gating. Hum. Mol. Genet. 30, 2300–2314. https://doi.org/10.1093/hmg/ddab192.

32. Lee, H., Lin, M.C.A., Kornblum, H.I., Papazian, D.M., and Nelson, S.F. (2014). Exome sequencing identifies de novo gain of function missense mutation in KCND2 in identical twins with autism and seizures that slows potassium channel inactivation. Hum. Mol. Genet. 23, 3481–3489. https://doi.org/10.1093/hmg/ddu056.

33. Lako, M., Lindsay, S., Bullen, P., Wilson, D.I., Robson, S.C., and Strachan, T. (1998). A novel mammalian wnt gene, WNT8B, shows brain-restricted expression in early development, with sharply delimited expression boundaries in the developing forebrain. Hum. Mol. Genet. 7, 813–822. https://doi.org/10.1093/hmg/7.5.813.

34. Grone, B.P., Marchese, M., Hamling, K.R., Kumar, M.G., Krasniak, C.S., Sicca, F., Santorelli, F.M., Patel, M., and Baraban, S.C. (2016). Epilepsy, Behavioral Abnormalities, and Physiological Comorbidities in Syntaxin-Binding Protein 1 (STXBP1) Mutant Zebrafish. PLoS One 11, e0151148. https://doi.org/10.1371/journal.pone.0151148.

35. Wu, R.S., Lam, I.I., Clay, H., Duong, D.N., Deo, R.C., and Coughlin, S.R. (2018). A Rapid Method for Directed Gene Knockout for Screening in G0 Zebrafish. Dev. Cell 46, 112–125.e4. https://doi.org/10.1016/j.devcel.2018.06.003.

36. Suls, A., Jaehn, J.A., Kecskés, A., Weber, Y., Weckhuysen, S., Craiu, D.C., Siekierska, A., Djémié, T., Afrikanova, T., Gormley, P., et al. (2013). De novo loss-of-function mutations in CHD2 cause a fever-sensitive myoclonic epileptic encephalopathy sharing features with Dravet syndrome. Am. J. Hum. Genet. 93, 967–975. https://doi.org/10.1016/j.ajhg.2013.09.017.

37. Hoffman, E.J., Turner, K.J., Fernandez, J.M., Cifuentes, D., Ghosh, M., Ijaz, S., Jain, R.A., Kubo, F., Bill, B.R., Baier, H., et al. (2016). Estrogens Suppress a Behavioral Phenotype in Zebrafish Mutants of the Autism Risk Gene, CNTNAP2. Neuron 89, 725–733. https://doi.org/10.1016/j.neuron.2015.12.039.

38. Robens, B.K., Yang, X., McGraw, C.M., Turner, L.H., Robens, C., Thyme, S., Rotenberg, A., and Poduri, A. (2022). Mosaic and non-mosaic protocadherin 19 mutation

leads to neuronal hyperexcitability in zebrafish. Neurobiol. Dis. 169, 105738. https://doi.org/10.1016/j.nbd.2022.105738.

39. Sun, X., and Lin, Y. (2016). Npas4: Linking Neuronal Activity to Memory. Trends Neurosci. 39, 264–275. https://doi.org/10.1016/j.tins.2016.02.003.

40. El-Brolosy, M.A., Kontarakis, Z., Rossi, A., Kuenne, C., Günther, S., Fukuda, N., Kikhi, K., Boezio, G.L.M., Takacs, C.M., Lai, S.L., et al. (2019). Genetic compensation triggered by mutant mRNA degradation. Nature 568, 193–197. https://doi.org/10.1038/s41586-019-1064-z.

41. El-Brolosy, M.A., and Stainier, D.Y.R. (2017). Genetic compensation: A phenomenon in search of mechanisms. PLoS Genet. 13, e1006780. https://doi.org/10.1371/journal.pgen.1006780.

42. Rossi, A., Kontarakis, Z., Gerri, C., Nolte, H., Hölper, S., Krüger, M., and Stainier, D.Y.R. (2015). Genetic compensation induced by deleterious mutations but not gene knockdowns. Nature 524, 230–233. https://doi.org/10.1038/nature14580.

43. Ma, Z., Zhu, P., Shi, H., Guo, L., Zhang, Q., Chen, Y., Chen, S., Zhang, Z., Peng, J., and Chen, J. (2019). PTC-bearing mRNA elicits a genetic compensation response via Upf3a and COMPASS components. Nature 568, 259–263. https://doi.org/10.1038/s41586-019-1057-y.

44. Jiang, L., and Wang, X. (2022). The miR-133b/brefeldin A-inhibited guanine nucleotide-exchange protein 1 (ARFGEF1) axis represses proliferation, invasion, and migration in cervical cancer cells. Bioengineered 13, 3323–3332. https://doi.org/10.1080/21655979.2022.2027063.

45. Liu, Y., Wu, D., Cheng, H., Chen, L., Zhang, W., Zou, L., Gao, Q., Zhao, Z., Chen, Q., Zeng, W., et al. (2021). Wnt8B, transcriptionally regulated by ZNF191, promotes cell proliferation of hepatocellular carcinoma via Wnt signaling. Cancer Sci. 112, 629–640. https://doi.org/10.1111/cas.14738.

46. Thyme, S.B., Pieper, L.M., Li, E.H., Pandey, S., Wang, Y., Morris, N.S., Sha, C., Choi, J.W., Herrera, K.J., Soucy, E.R., et al. (2019). Phenotypic Landscape of Schizophrenia-Associated Genes Defines Candidates and Their Shared Functions. Cell 177, 478–491.e20. https://doi.org/10.1016/j.cell.2019.01.048.

47. Harper, C., and Lawrence, C. (2016). In The Laboratory Zebrafish, 1st ed.

48. Labun, K., Montague, T.G., Krause, M., Torres Cleuren, Y.N., Tjeldnes, H., and Valen, E. (2019). CHOPCHOP v3: expanding the CRISPR web toolbox beyond genome editing. Nucleic Acids Res 47, W171–W174. https://doi.org/10.1093/nar/gkz365.

49. Amzica, F., and Steriade, M. (1999). Spontaneous and artificial activation of neocortical seizures. J. Neurophysiol. 82, 3123–3138. https://doi.org/10.1152/jn.1999.82.6.3123.

STAR★METHODS

KEY RESOURCES TABLE

REAGENT or RESOURCE	SOURCE	IDENTIFIER
Chemicals, peptides, and recombinant proteins		
TrueCut™ Cas9 Protein v2	Invitrogen	Cat #: A36496
Pentylenetetrazole (PTZ)	Sigma-Aldrich	Cat #: P6500-25G
Instant Ocean® Sea Salt	Instant Ocean	Cat #: SS3-50 - 50
Methylene Blue	Sigma-Aldrich	Cat #: PHR3838-1G
alpha-bungarotoxin	Sigma-Aldrich	Cat #: B13422
Low melting point agarose	Fisher Scientific	Cat #: BP165-25
RNAlater™ Stabilization Solution	Thermo-fisher	Cat #: AM7020
RNeasy plus kit	Qiagen	Cat #: 74134
Deposited data		
RNA-Seq data	This paper	PRJNA1111077
Experimental models: Organisms/strains		
Zebrafish: AB WT	ZIRC	RRID:ZIRC_ZL1
Zebrafish: cnnm2a/b	Thyme et al.[46]	N/A
Zebrafish: dlx6a-1.4kbdlx5a/dlx6a: GFP:vglut2:dsRed	Robens et al.[38]	N/A
Oligonucleotides		
sgRNA kits (See Table S1 for Oligonucleotides)	Synthego	https://www.synthego.com/order/ crispr-kits/synthetic-sgrna
Primers (See Table S1 for Oligonucleotides)	Invitrogen	https://www.thermofisher.com/us/en/ home/life-science/oligonucleotides-primers- probes-genes/custom-dna-oligos.html
Software and algorithms		
EpiGad	Susceptibility Genes	https://www.epigad.org/
Carpedb	Caldwell Lab	http://carpedb.ua.edu/search.cfm
CHOPCHOP	Labun et al.[47]	https://chopchop.cbu.uib.no/
Ethovision Xt	Noldus	https://www.noldus.com/ethovision-xt
pClamp 11	Molecular devices	https://www.moleculardevices.com/products/ axon-patch-clamp-system/acquisition-and- analysis-software/pclamp-software-suite
Zen 3.4 (blue edition)	Zeiss	https://www.zeiss.com/microscopy/en/ products/software/light-microscopy- software.html
ImageJ	ImageJ (version 2.1.0)	https://imagej.net/ij/download.html
R	R version 4.0.0	https://cran.r-project.org/bin/windows/base/old/
OMIM	McKusick-Nathans Institute of Genetic Medicine, The Johns Hopkins University School of Medicine	https://www.omim.org/
ICE CRISPR Analysis Tool	Synthego	https://ice.synthego.com/#/
MATLAB	MathWorks	https://www.mathworks.com/ products/matlab/student.html
Zebrafish-LFP	Github	https://doi.org/10.5281/zenodo.11165681

(Continued on next page)

Continued		
REAGENT or RESOURCE	SOURCE	IDENTIFIER
Zebrafish-Neuron-Counter	Github	https://doi.org/10.5281/zenodo.11166076
Zebrafish-RNAseq	Github	https://doi.org/10.5281/zenodo.11165954

RESOURCE AVAILABILITY

Lead contact

Further information and request for materials should be directed to and will be fulfilled by the Lead Contact, Annapurna Poduri (annapurna.poduri@childrens.harvard.edu).

Materials availability

Zebrafish lines generated in this study are available by request of the lead contact and Cryogenetics Inc.

Data and code availability

- RNA-Seq data have been deposited at SRA and is publicly available as of the date of the publication. Accession number is listed in the key resources table.
- All original code has been deposited at Zenodo and is publicly available as of the date of publication. DOIs are listed in the key resources table.
- Any additional information required to reanalyze any data reported in this paper will be made available from the lead contact upon request.

EXPERIMENTAL MODEL AND STUDY PARTICIPANT DETAILS

Initial screen microinjections involved an estimated 13,300 zebrafish embryos in the background strain TAB (RRID:ZIRC_ZL1). Estimation was calculated based on screen guide iterations (133) and the target of ~100 animals per injection round. Guide iterations were calculated to include all paralogous duplicates injected individually and co-injected. F_0 mutants successfully outcrossed led to approximately 8,600 F_1 fish (86 guide iterations and ~100 embryos per clutch). Mutants cnnm2a and cnnm2b were not generated by injection, but were imported into the lab as stable as HET line[46] (generous donation from Dr. Summer Thyme, University of Massachusetts Chan Medical School). A subset of stable F2 mutants were crossed into transgenic tg(dlx6a-1.4kbdlx5a/dlx6a: GFP::vglut2:dsRed) (generous donation from Dr. Ellen Hoffman, Yale University).[38] A total of 7,786 F_2 larvae were assayed for behavioral screening, 164 larvae for local field potential recordings and 150 larvae for interneuron counting. A total of 90 larvae (10 larval heads pooled and run-in triplicate for 3 genes) were used for RNA-Seq. Sex of assayed animals is irrelevant to analysis because all experimentation was conducted prior to the age of zebrafish sex determination.

Larvae were kept in 100mL Petri dishes in sterile fish water (SFW) (60 mg/mL Instant Ocean Sea Salt) with 0.0002% methylene blue at a density of fewer than 100 embryos per plate. Methylene blue SFW was cleared at 1 dpf and replaced with 100% SFW before larval chorion shedding.[47] Larvae were maintained with daily replacement of SFW in an incubator with a 14-10-h light-dark cycle at 26C until the date of experimentation. All zebrafish experimental procedures were approved by the Boston Children's Hospital Institutional Animal Care and Use Committee.

METHOD DETAILS

Generating a candidate epilepsy gene list

Genes possibly associated with epilepsy were identified from the literature, using PubMed keywords "epilepsy," "seizure," and "gene" and published data from the Epi4K Consortium5 and other databases, including EpiGad, Carpedb, and OMIM. Gene lists obtained from a compendium of clinical genetic labs (https://www.ncbi.nlm.nih.gov/gtr/) were also included. After removing duplicates, a list of unique "candidate epilepsy genes" was consolidated and evaluated by the neurologists and genetic counselors of the Boston Children's Hospital (BCH) Epilepsy Genetics Program.

CRISPR guide design

We used the CRISPR/Cas9 system to disrupt the function of the zebrafish gene paralogs of the 81 candidate epilepsy genes described above. CRISPR/Cas9 sgRNA guides were designed to introduce out-of-frame deletions predicted to result in premature terminating codons (PTC) of target genes via non-homologous end-joining. Two sets of CRISPR/Cas9 guides were designed near the 5′ and 3′ ends for each transcript, excluding the first exon and last exon, respectively. Designs for duplicated genes included two sets of guides per paralog (e.g., atp1a3a and atp1a3b). Target sites were selected on different exons across the entire length of each non-overlapping gene transcript using CHOPCHOP.[48] Guide requirements included targeting efficiency >50% based upon high GC content and minimal self-complementary within the sgRNA, or between the sgRNA and RNA backbone. Additional requirements included no-off target matches and a Protospacer Adjacent Motif (PAM)

sequence (nucleotides NGG) upstream of the desired target (Table S1). All guides (sgRNA kits) were generously donated by Synthego (Redwood City, CA, USA).

Generation of stable zebrafish mutants

Zebrafish embryos were injected at the 1-cell stage with 500 pg/nL sgRNA and 500 pg/nL TrueCut Cas9 Protein v2. Mosaic F0 larvae were raised to breeding age (2–3 months) in 2.8L tanks containing fewer than 30 zebrafish and outcrossed to a WT casper transparent line. All F_0 founders were genotyped via Sanger sequencing (PCR) from fin-clipped tissue samples and individually outcrossed to WT, which generated half WT and half HET F_1 offspring. Germline transmission of CRISPR indels was assessed via genotyping pools of 5 2 dpf F_1 TAB larvae from isolated F0 parents, while remaining F_1 clutches were housed pending genotyping results. Mutant allele-containing F_1 fish were raised to breeding age and fin-clipped for DNA to assess for HET mutants. Indel and frameshift mutation predictions was conducted by the Synthego ICE CRISPR Analysis Tool. F_1 ICE analysis allowed mutant genotypes to be differentiated in cases of mosaic indels in F_0 germline. Genotyping of individual or pooled larvae was conducted by Sanger sequencing from Genewiz and DNA was extracted by standard methods. A single INDEL was chosen for each targeted paralog and those F_1 HETs were in-crossed for F_2 behavior paradigms and additional assays. Single mutations were preferentially chosen for each line based on their predicted likelihood to be truncating and result in nonsense-mediated decay. This was in attempt to avoid gain-of-function mutations, which are typically the result of single nucleotide changes, and polymorphisms. HET F_3 transgenic fish were sorted for loss of pigment, maximum fluorescence and genotyped.

Zebrafish behavior paradigms

F2 5dpf larvae were placed in an automated motion tracking system (DanioVision, Noldus, Wageningen, Netherlands), allowed to acclimate for 5 min and then evaluated in three conditions: (a) 1 h of recording spontaneous activity, (b) a 26-min light paradigm consisting of four oscillating periods of dark and flashing light (2hz–10hz with a 2hz increase per light interval, a paradigm adapted from human EEG methods to detect photosensitivity,[49] and (c) 30 min in subthreshold PTZ paradigm (adding 100 µl per well PTZ well for a final concentration of 0.125 mM). Subthreshold concentration was determined by the highest PTZ concentration at which no SII events were observed in WT larvae during a 30-min PTZ titration trial. Motion detection assays were conducted in duplicate for each gene. Assayed larvae were generated from HET x HET in-crosses to provide internal WT controls and assess for batch effects. After screening ~20,000 larvae, a list of the most promising candidates for a potential seizure model was developed. Criteria were developed based on SII stereotypical seizure-like swim patterns found in PTZ-treated larvae, as described.[17]

Local field potential recording

Electrophysiological studies were conducted using a modified version of established published methods.[17] 5–6 dpf larval zebrafish were treated with 2 mg/mL alpha-bungarotoxin for 10 min and embedded in 2% low melting point (LMP) agarose to eliminate movement. Embedded fish were perfused with artificial CSF containing 117 mM NaCl, 4.7 mM KCl, 2.5 mM NaHCO3, 2.5 mM CaCl2, 1.2 mM MgCl2, 1.2 mM NaH2PO4, 11 mM glucose throughout the recording. A glass microelectrode was placed in the optic tectum, the largest forebrain region in the zebrafish. Electrodes (1–7 MΩ) were backloaded with 2 M NaCl prior to placement. Electrical activity was recorded using pClamp 11 software, and an Axopatch 200B amplifier (Axon Instruments, Union City, CA, USA). Voltage records were low-pass filtered at 1 kHz (3 dB; eight-pole Bessel), high-pass filtered at 0.1–0.2 Hz, digitized at 5–10 kHz using a Digidata 1440A interface. Proper electrode positioning and detection of physiological activity was detected with the addition of PTZ at the end of each recording and data corresponding to animals failing to respond to proconvulsant was disregarded.

Imaging

Confocal imaging: F3 tg(*dlx6a-1.4kbdlx5a/dlx6a:GFP::vglut2:dsRed*) HET larvae were crossed and sorted to maximize fluorescence and pigmentation loss. 5 dpf larvae were fixed in 4% PFA overnight and stored in PBS at 4C. Larvae were dorsally mounted in 100 µl 1.2 LMP agarose. Imaging was conducted on a Zeiss LSM700 at 10x magnification with a 10 µm step size. Image analysis was conducted using Fiji software, and GFP-expressing interneurons were quantified using a custom macro (https://doi.org/10.5281/zenodo.11166076) as described previously.[38] Fluorescence intensity was normalized between samples with a cutoff threshold of 99% greater than background.

RNA-Seq preparation

Three replicate larvae from Het in-crosses, aged 5 dpf, were sacrificed on ice and stored in RNAlater Stabilization Solution according to product specifications. Larval heads were isolated from bodies, which were used for Sanger sequencing for genotyping. Heads were pooled in groups of 20–25 according to genotype and RNA was isolated using a Qiagen RNeasy plus kit according to specifications. QC was performed via Agilent 2100 bioanalyzer, and only samples with an RNA integrity number value of >5.8 were used for library preparation. Sequencing was performed using an Illumina NovaSeq 6000 Sequencing System with >20 million reads per sample.

QUANTIFICATION AND STATISTICAL ANALYSIS

Qualification and analysis of swim behavior

Motion tracking data were analyzed using Ethovision Xt software. SI seizure events were defined by significant increase in the Ethovision parameters "average velocity," "average distance" compared to WT controls. SII seizures were identified by auto-detection of "total distance" (TD) > 60mm and "velocity max" (VM) > 90 mm/s, evaluating data from 5-s bins; seizure events were confirmed by visual inspection by a trained researcher. We calculated the binomial probability of the proportion of mutant larvae displaying SII events compared to proportion of the number of WT displaying SII events (Table S2). Initial population probability of spontaneous WT SII behavior was determined (0.023) from ∼400 uninjected TAB larvae. Population probability was further refined after incorporating WT sibling controls WTs from a subsequent series of genotyping performed on any gene with significantly higher binomial probability of larvae with >0 SII events given suspected Medellin inheritance with the WT population proportion of 0.023. From this cohort, a new proportion of WT > 0 SII event was updated to a frequency of 0.027. The updated WT sibling controls WT genotype SII swim data was then incorporated into the population probability for binomial significance assessment in the PTZ and light-provoked paradigms to be use as the threshold for behavior screening. These evaluations were conducted blind to genotype, and post hoc, larvae were sacrificed by standard freezing methods and genotyped via Sanger sequencing.

Local field potential analysis

Custom MATLAB code (https://doi.org/10.5281/zenodo.11165681) was used to analyze local field potential. Raw data were normalized using a root-mean-square (RMS) method, band-pass filtered at 3-10Hz to detect events in the physiological 100-300msec range and then smoothed with a 200-msec boxcar moving average filter. For display, the spike amplitude was normalized, and the "instantaneous spike rate" was computed by summation of spikes in a 20-s moving window. Spikes were defined as deflections exceeding the interquartile range (IQR) of filtered voltage values by 2x within a 10-s moving window (1000 samples). The peak of a "spike" was defined as exceeding 6X the moving IQR. Spike counts between all genotypes ranged from >100 to ∼500 within recording window with median amplitudes from 0.05 to 0.4. Additionally, mutants displayed an increase in deflection clusters and durations. Burst were defined as greater than 3 spikes for longer than a second at a rate exceeding .3hz. Bursting event counts within all genotypes ranged between 0 and 30 within analysis window counts with durations ranging from 0 to 1000 s.

RNA-Seq analysis

A custom pipeline was used for RNA-Seq analysis. Sequencing data were aligned to zebrafish genome danRer11 using STAR. Expression was quantified using featureCounts. For each group of HET, HOM and WT sibling controls WT samples, only protein-coding genes with transcript per million value ≥ 1 in at least 2 samples were retained for downstream analysis. RUVSeq (RUVr k = 2, v1.28.0) was used to remove batch effect; differential gene expression analysis was then performed using DESeq2 (v2.28.0). Differentially expressed genes were defined as those with absolute log2 fold change >1 and adjusted $p < 0.05$. Gene Ontology (GO) enrichment analysis was performed using clusterProfiler (v4.7.0). The following files are available on Github (https://doi.org/10.5281/zenodo.11165954): 'DEG_identification.R', Code for RUVr batch effect correction and DEG identification; 'pathway_analysis.R', code for pathway analysis (KEGG + GO); 'functions.R', functions used by the above scripts.